SSD-TR-90-50

(12)

AEROSPACE REPORT NO.
TR-0090(5604)-2

AD-A231 365

Calculation of the NFb$^1\Sigma$ - X$^3\Sigma^-$ Stimulated Emission Cross Section

Prepared by

J. B. KOFFEND
Aerophysics Laboratory
Laboratory Operations

29 November 1990

Prepared for

WEAPONS LABORATORY
Kirtland Air Force Base, NM 87117

SPACE SYSTEMS DIVISION
AIR FORCE SYSTEMS COMMAND
Los Angeles Air Force Base
P. O. Box 92960
Los Angeles, CA 90009-2960

Development Group

THE AEROSPACE CORPORATION
El Segundo, California

This report was submitted by The Aerospace Corporation, El Segundo, CA 90245-4691, under Contract No. F04701-88-C-0089 with the Space Systems Division, P.O. Box 92960, Los Angeles, CA 90009-2960. It was reviewed and approved for The Aerospace Corporation by R. W. Fillers, Director, Aerophysics Laboratory. Captain Riviere was the project officer.

This report has been reviewed by the Public Affairs Office (PAS) and is releasable to the National Technical Information Service (NTIS). At NTIS, it will be available to the general public, including foreign nationals.

This technical report has been reviewed and is approved for publication. Publication of this report does not constitute Air Force approval of the report's findings or conclusions. It is published only for the exchange and stimulation of ideas.

RAFAEL A. RIVIERE, Capt, USAF
MOIE Project Officer
SSD/CNL

JONATHAN M. EMMES, MAJ, USAF
MOIE Project Manager
AFSTC/WCO OL-AB

UNCLASSIFIED

SECURITY CLASSIFICATION OF THIS PAGE

REPORT DOCUMENTATION PAGE

1a. REPORT SECURITY CLASSIFICATION Unclassified	1b. RESTRICTIVE MARKINGS
2a. SECURITY CLASSIFICATION AUTHORITY	3. DISTRIBUTION/AVAILABILITY OF REPORT Approved for public release; distribution unlimited.
2b. DECLASSIFICATION/DOWNGRADING SCHEDULE	
4. PERFORMING ORGANIZATION REPORT NUMBER(S) TR-0090(5604)-2	5. MONITORING ORGANIZATION REPORT NUMBER(S) SSD-TR-90-50
6a. NAME OF PERFORMING ORGANIZATION The Aerospace Corporation Laboratory Operations 6b. OFFICE SYMBOL (If applicable)	7a. NAME OF MONITORING ORGANIZATION Space Systems Division
6c. ADDRESS (City, State, and ZIP Code) El Segundo, CA 90245-4691	7b. ADDRESS (City, State, and ZIP Code) Los Angeles Air Force Base Los Angeles, CA 90009-2960
8a. NAME OF FUNDING/SPONSORING ORGANIZATION 8b. OFFICE SYMBOL (If applicable)	9. PROCUREMENT INSTRUMENT IDENTIFICATION NUMBER F04701-88-C-0089
8c. ADDRESS (City, State, and ZIP Code)	10. SOURCE OF FUNDING NUMBERS PROGRAM ELEMENT NO. / PROJECT NO. / TASK NO. / WORK UNIT ACCESSION NO.

11. TITLE (Include Security Classification)

Calculation of the $NFb\,^1\Sigma - X\,^3\Sigma^-$ Stimulated Emission Cross Section

12. PERSONAL AUTHOR(S)

Koffend, J. B.

13a. TYPE OF REPORT	13b. TIME COVERED	14. DATE OF REPORT (Year, Month, Day)	15. PAGE COUNT
	FROM ____ TO ____	1990 November 29	17

16. SUPPLEMENTARY NOTATION

17. COSATI CODES			18. SUBJECT TERMS (Continue on reverse if necessary and identify by block number)
FIELD	GROUP	SUB-GROUP	Nuclear Motion Electronic Motion

19. ABSTRACT (Continue on reverse if necessary and identify by block number)

The stimulated emission cross section for the $NFb\,^1\Sigma - X\,^3\Sigma^-$ transition has been derived under conditions of the Born-Oppenheimer approximation where coordinates involving nuclear and electronic motion are separable. Exact and Hund's coupling case B Hönl-London factors are presented. Sample calculations for the five rotational branches of the $NFb\,^1\Sigma - X\,^3\Sigma^-(0,0)$ band at several temperatures are given.

Availability Codes	
Dist	Avail and/or Special
A-1	

20. DISTRIBUTION/AVAILABILITY OF ABSTRACT ☒ UNCLASSIFIED/UNLIMITED ☐ SAME AS RPT. ☐ DTIC USERS	21. ABSTRACT SECURITY CLASSIFICATION Unclassified
22a. NAME OF RESPONSIBLE INDIVIDUAL	22b. TELEPHONE (Include Area Code) / 22c. OFFICE SYMBOL

DD FORM 1473, 84 MAR — 83 APR edition may be used until exhausted. All other editions are obsolete.

SECURITY CLASSIFICATION OF THIS PAGE

UNCLASSIFIED

The stimulated emission cross section for a transition between an initial state $<I|$ and a final state $|F>$ is given by:

$$\sigma_{em}(\nu) = (8\pi^3/3ch)\ |<I|\mu|F>|^2\ \nu\ g(\nu), \tag{1}$$

where $|<I|\mu|F>|$ is the electric dipole matrix element connecting the two levels, ν is the frequency of the transition, and $g(\nu)$ is the normalized lineshape function.

For the NF $b^1\Sigma$ $-X^3\Sigma^-$ transition, we can write

$$|<I|\mu|F>|^2 = |<\mathrm{NF}\ b^1\Sigma,v',N'|\mu|\mathrm{NF}\ X^3\Sigma^-,v'',N''>|^2, \tag{2}$$

where v is the vibrational quantum number and N is the rotational quantum number. Under the Born–Oppenheimer approximation where coordinates involving nuclear and electronic motion are separable, Eq. (1) can be written as

$$|<I|\mu|F>|^2 = |R_e|^2\ q_{v'v''}\ s(N')/(2N'+1), \tag{3}$$

where $|R_e|^2$ is the electronic transition moment, $q_{v'v''}$ is the Franck–Condon factor, and $s(N')$ are Hönl–London factors which depend upon the rotational quantum number N'.

The NF $b^1\Sigma$ - $X^3\Sigma^-$ spectrum consists of the rotational branches depicted in Fig. 1. Although five branches are present, it should be noted that the much stronger ^QP and ^QR branches comprise most of the intensity for a particular set of transitions from a specific NF $b^1\Sigma,v',N'$ level. Following the notation given by Vervloet and Watson (Ref. 2), Eq. (3) becomes

$$|<I|\mu|F>|^2 = q_{v'v''}\ \mu_0^2\ s(N,\rho)/(2N'+1), \tag{4}$$

where μ_0^2 is the parallel electronic transition moment. The Hönl–London factors appearing in Eq (4) are given in Table 1. Two sets of Hönl–London factors are listed in Table 1. One set is valid for any $^3\Sigma$ - $^1\Sigma$ transition and the other is valid for Hund's coupling case b. It should be noted that the simpler Hund's case b factors may be used to a good level of approximation for the case of NF, since the spin–spin interaction constant for the NF $^3\Sigma^-$ state is small compared to the rotational energy level spacing (Refs. 2 and 3) even at relatively low N''. This trend is illustrated in Fig. 2, where relative Hönl–London factors for the ^QP branch are plotted as a function of N'. For a particular NF $(b^1\Sigma,v',N') \rightarrow$ NF $(X^3\Sigma^-\ v'',N'')$ transition, the stimulated emission cross section is

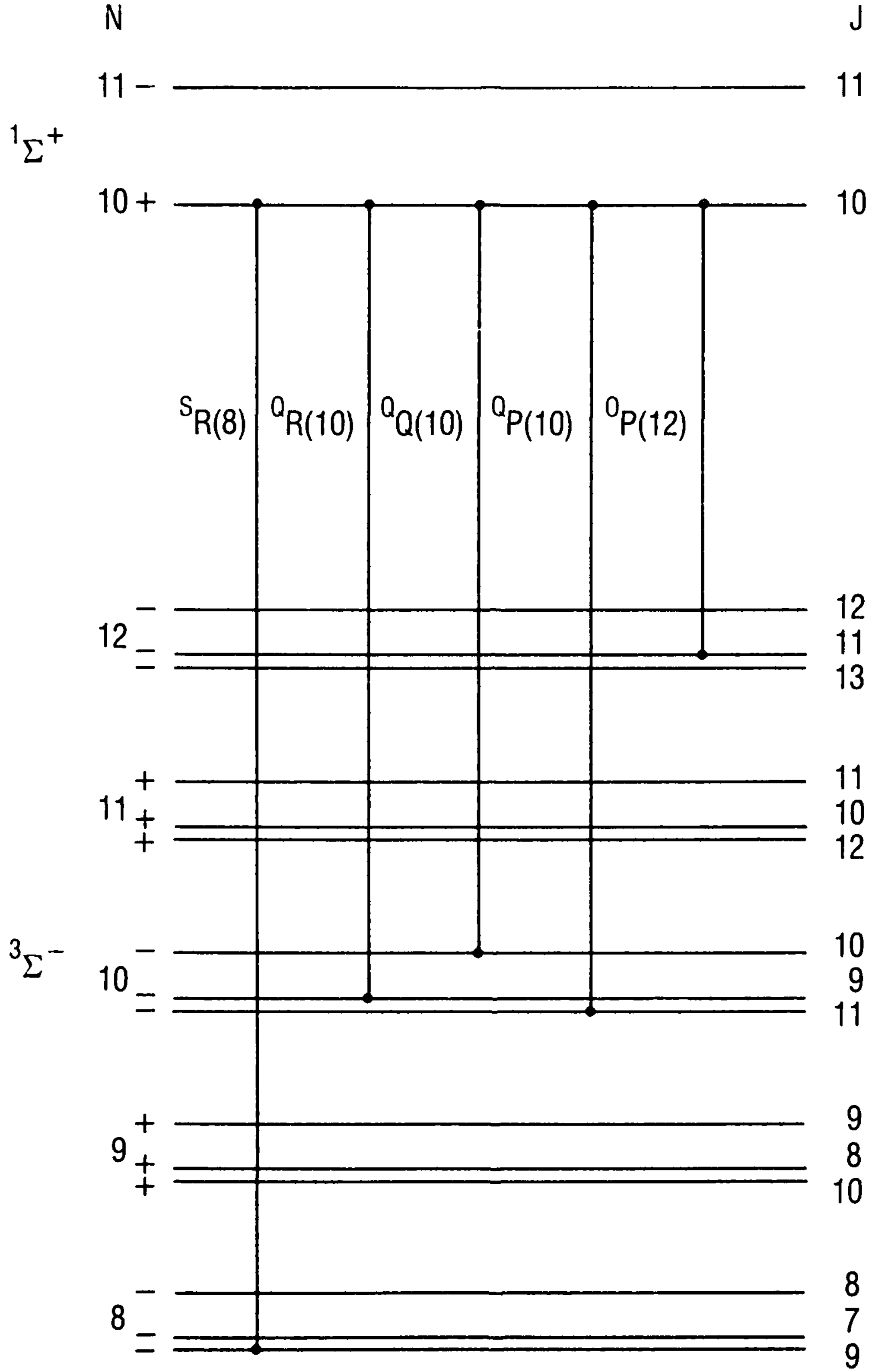

Fig. 1. Rotational Branches in a $^1\Sigma$ – $^3\Sigma^-$ Transition

Table 1. NF $b^1\Sigma$ - $X3\Sigma^-$ Hönl–London Factors

N	${}^{O}P$ Branch	${}^{Q}P$ Branch	${}^{Q}Q$ Branch	${}^{Q}R$ Branch	${}^{S}R$ Branch
${}^{O}P$	N–1	$[s_jJ^{1/2} - c_j(J+1)^{1/2}\rho]^2$		$\mu_0^2\, [(1-\rho)^2\, (N+1)\, (N+2)]/(2N+3)$	
${}^{Q}P$	N+1	$[c_jJ^{1/2} + s_j(J+1)^{1/2}\rho]^2$		$\mu_0^2\, [(N + (N-1)\rho]^2/(2N-1)$	
${}^{Q}Q$	N	$(2J+1)\rho^2$		$\mu_0^2\, (2N+1)\rho^2$	
${}^{Q}R$	N–1	$[s_j(J+1)^{1/2} + c_jJ^{1/2}\rho]^2$		$\mu_0^2\, [(N+1) + (N+2)\rho]^2/(2N+3)$	
${}^{S}R$	N+1	$[c_j(J+1)^{1/2} - s_jJ^{1/2}\rho]^2$		$\mu_0^2\, (1-\rho)^2\, (N-1)\, N]/(2N+3)$	

[a]N is the NF $b^1\Sigma$ rotational quantum number.
[b]$\rho = \mu_1/\mu_0$
[c]$s_j = \{[(F_2(J)-F_1(J)]/[F_3(J)-F_1(J)]\}^{1/2}$
$c_j = \{[(F_3(J)-F_2(J)]/[F_3(J)-F_1(J)]\}^{1/2}$
$F_1(J) = B\,J(J+1) + (B - \lambda - \gamma/2) - [(B - \lambda - \gamma/2)^2 + 4J(J+1)(B - \gamma/2)^2]^{1/2}$
$F_2(J) = B\,J(J+1)$
$F_3(J) = B\,J(J+1) + (B - \lambda - \gamma/2) + [(B - \lambda - \gamma/2)^2 + 4J(J+1)(B - \gamma/2)^2]^{1/2}$

$$\sigma_{em}(\nu) = (8\pi^3/3ch)\, q_{v'v''}\, \mu_0^2\, s(N',\rho)/(2N'+1)\, g(\nu). \qquad (5)$$

<u>Sample Calculations</u>

Tables 2–4 contain calculated stimulated emission cross sections for the five branches of the NF $b^1\Sigma$ - $X^3\Sigma^-$ (0,0) band at several temperatures using Eq. (5). The full Hönl–London factors rather than the Hund's case b limit were used in the calculations. The values represent cross sections at the peak of Doppler–broadened lines whose normalized lineshape function is

$$g(\nu) = (2(\ln 2/\pi)^{1/2})/\Delta\nu_D\, \exp[(-4\ln 2\, (\nu-\nu_o)^2)/\Delta\nu_D^2], \qquad (6)$$

where $\Delta\nu_D$ is the FWHM Doppler width and ν_o is the frequency at line center. The Doppler width is given by

$$\Delta\nu_D = 2\nu_o\, (2kT\ln 2/Mc^2)^{1/2}, \qquad (7)$$

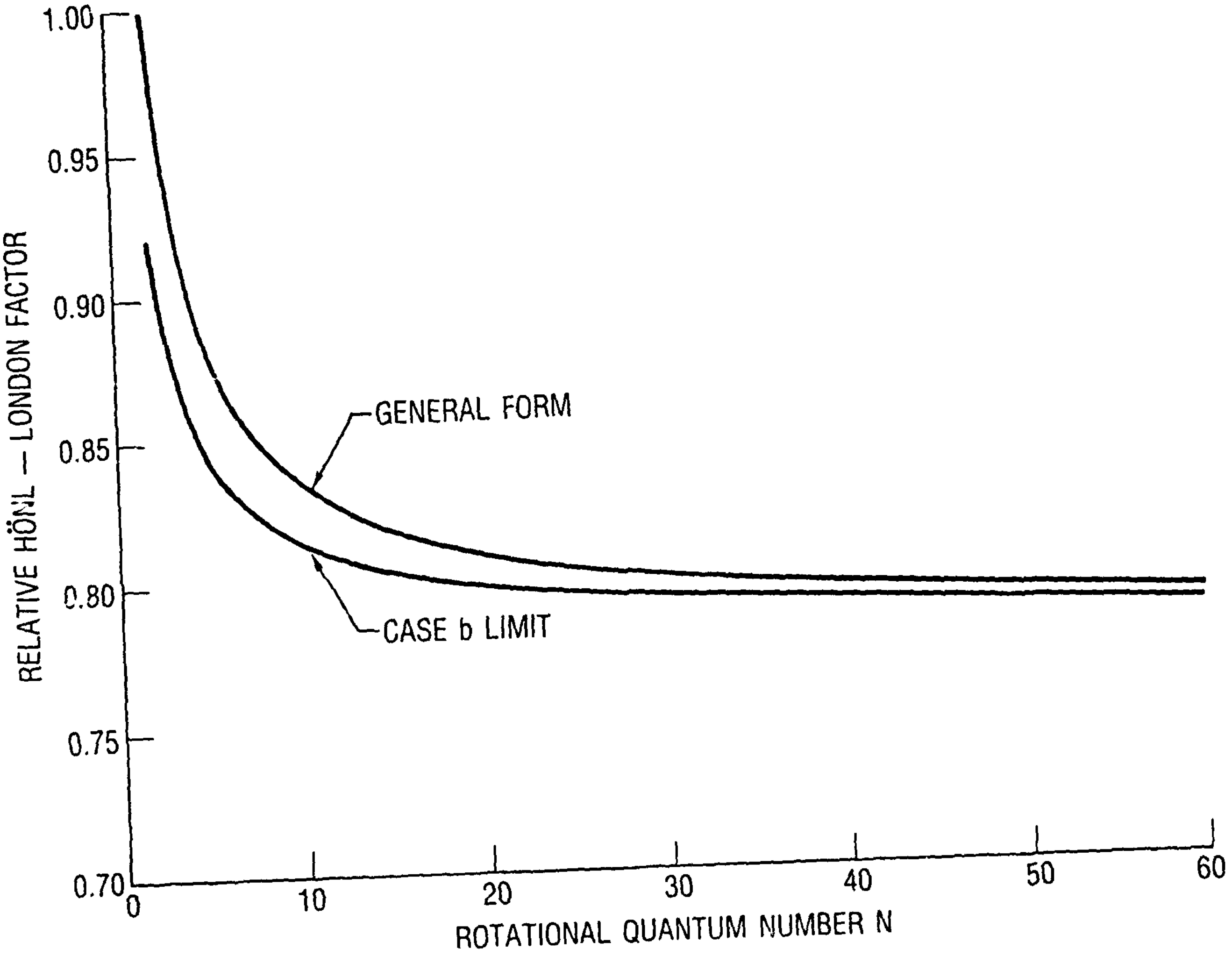

Fig.2 $^1\Sigma$ - $^3\Sigma^-$ Hönel-London Factors Plotted vs N

where M is the mass of the species. Values of $\mu_0 = 2.72 \times 10^6 \, (ea_o)^2$ and $\mu_1/\mu_o = 0.2611$ used in the calculations as well as the NF $X^3\Sigma^-$ state spectroscopic constants were taken from Ref. 2. Note that the values in Tables 2–4 represent stimulated emission cross sections per NF molecule in a particular $b^1\Sigma^-$ rotational level in $v'=0$. The small signal gain for a unit length of gain medium is given by

$$\text{gain} = \sigma([\text{NF } b^1\Sigma, v'=0, N'] - (1/3)[\text{NF } X^3\Sigma^-, v''=0, J'']). \tag{8}$$

The factor of 1/3 appearing in Eq. (8) comes from the fact that the degeneracy of the NF $X^3\Sigma^-$ state is three while the NF $b^1\Sigma$ has a degeneracy of one.

Table 2. Calculated NF b–X (0,0) Band Stimulated Emission Cross Section at 300 K

N	^{O}P Branch	^{Q}P Branch	^{Q}Q Branch	^{Q}R Branch	^{S}R Branch
2	1.202×10^{-19}	1.519×10^{-18}	2.040×10^{-19}	8.426×10^{-19}	7.148×10^{-19}
3	1.988×10^{-19}	1.426×10^{-18}	2.040×10^{-19}	9.454×10^{-19}	6.264×10^{-19}
4	2.442×10^{-19}	1.374×10^{-18}	2.040×10^{-19}	1.001×10^{-18}	5.776×10^{-19}
5	2.735×10^{-19}	1.341×10^{-18}	2.040×10^{-19}	1.036×10^{-18}	5.466×10^{-19}
6	2.940×10^{-19}	1.318×10^{-18}	2.040×10^{-19}	1.060×10^{-18}	5.252×10^{-19}
7	3.091×10^{-19}	1.301×10^{-18}	2.040×10^{-19}	1.077×10^{-18}	5.095×10^{-19}
8	3.207×10^{-19}	1.288×10^{-18}	2.040×10^{-19}	1.091×10^{-18}	4.976×10^{-19}
9	3.298×10^{-19}	1.277×10^{-18}	2.040×10^{-19}	1.101×10^{-18}	4.882×10^{-19}
10	3.373×10^{-19}	1.269×10^{-18}	2.040×10^{-19}	1.110×10^{-18}	4.805×10^{-19}
11	3.434×10^{-19}	1.262×10^{-18}	2.040×10^{-19}	1.117×10^{-18}	4.742×10^{-19}
12	3.486×10^{-19}	1.257×10^{-18}	2.040×10^{-19}	1.123×10^{-18}	4.690×10^{-19}
13	3.530×10^{-19}	1.252×10^{-18}	2.040×10^{-19}	1.128×10^{-18}	4.645×10^{-19}
14	3.568×10^{-19}	1.247×10^{-18}	2.040×10^{-19}	1.132×10^{-18}	4.606×10^{-19}
15	3.601×10^{-19}	1.244×10^{-18}	2.040×10^{-19}	1.136×10^{-18}	4.572×10^{-19}
16	3.630×10^{-19}	1.240×10^{-18}	2.040×10^{-19}	1.139×10^{-18}	4.542×10^{-19}
17	3.656×10^{-19}	1.238×10^{-18}	2.040×10^{-19}	1.142×10^{-18}	4.516×10^{-19}
18	3.679×10^{-19}	1.235×10^{-18}	2.040×10^{-19}	1.144×10^{-18}	4.493×10^{-19}
19	3.700×10^{-19}	1.233×10^{-18}	2.040×10^{-19}	1.147×10^{-18}	4.472×10^{-19}
20	3.719×10^{-19}	1.231×10^{-18}	2.040×10^{-19}	1.149×10^{-18}	4.453×10^{-19}
21	3.736×10^{-19}	1.229×10^{-18}	2.040×10^{-19}	1.151×10^{-18}	4.436×10^{-19}
22	3.751×10^{-19}	1.227×10^{-18}	2.040×10^{-19}	1.153×10^{-18}	4.420×10^{-19}
23	3.765×10^{-19}	1.225×10^{-18}	2.040×10^{-19}	1.154×10^{-18}	4.406×10^{-19}
24	3.778×10^{-19}	1.224×10^{-18}	2.040×10^{-19}	1.156×10^{-18}	4.393×10^{-19}
25	3.790×10^{-19}	1.223×10^{-18}	2.040×10^{-19}	1.157×10^{-18}	4.381×10^{-19}
26	3.801×10^{-19}	1.221×10^{-18}	2.040×10^{-19}	1.158×10^{-18}	4.369×10^{-19}
27	3.812×10^{-19}	1.220×10^{-18}	2.040×10^{-19}	1.159×10^{-18}	4.359×10^{-19}
28	3.821×10^{-19}	1.219×10^{-18}	2.040×10^{-19}	1.160×10^{-18}	4.349×10^{-19}
29	3.830×10^{-19}	1.218×10^{-18}	2.040×10^{-19}	1.161×10^{-18}	4.340×10^{-19}
30	3.839×10^{-19}	1.217×10^{-18}	2.040×10^{-19}	1.162×10^{-18}	4.332×10^{-19}

Table 2. Calculated NF b–X (0,0) Band Stimulated Emission Cross Section at 300 K (continued)

N	^{O}P Branch	^{Q}P Branch	^{Q}Q Branch	^{Q}R Branch	^{S}R Branch
31	3.846×10^{-19}	1.216×10^{-18}	2.040×10^{-19}	1.163×10^{-18}	4.324×10^{-19}
32	3.854×10^{-19}	1.216×10^{-18}	2.040×10^{-19}	1.164×10^{-18}	4.317×10^{-19}
33	3.861×10^{-19}	1.215×10^{-18}	2.040×10^{-19}	1.165×10^{-18}	4.310×10^{-19}
34	3.867×10^{-19}	1.214×10^{-18}	2.040×10^{-19}	1.166×10^{-18}	4.303×10^{-19}
35	3.873×10^{-19}	1.213×10^{-18}	2.040×10^{-19}	1.166×10^{-18}	4.297×10^{-19}
36	3.879×10^{-19}	1.213×10^{-18}	2.040×10^{-19}	1.167×10^{-18}	4.291×10^{-19}
37	3.884×10^{-19}	1.212×10^{-18}	2.040×10^{-19}	1.168×10^{-18}	4.286×10^{-19}
38	3.890×10^{-19}	1.212×10^{-18}	2.040×10^{-19}	1.168×10^{-18}	4.281×10^{-19}
39	3.895×10^{-19}	1.211×10^{-18}	2.040×10^{-19}	1.169×10^{-18}	4.276×10^{-19}
40	3.899×10^{-19}	1.210×10^{-18}	2.040×10^{-19}	1.169×10^{-18}	4.271×10^{-19}

Cross section in units of cm3/molecule

Table 3. Calculated NF b–X (0,0) Band Stimulated Emission Cross Section at 600 K

N	^{O}P Branch	^{Q}P Branch	^{Q}Q Branch	^{Q}R Branch	^{S}R Branch
2	8.502×10^{-20}	1.074×10^{-18}	1.443×10^{-19}	5.958×10^{-19}	5.054×10^{-19}
3	1.406×10^{-19}	1.008×10^{-18}	1.443×10^{-19}	6.685×10^{-19}	4.430×10^{-19}
4	1.727×10^{-19}	9.715×10^{-19}	1.443×10^{-19}	7.078×10^{-19}	4.084×10^{-19}
5	1.934×10^{-19}	9.480×10^{-19}	1.443×10^{-19}	7.324×10^{-19}	3.865×10^{-19}
6	2.079×10^{-19}	9.317×10^{-19}	1.443×10^{-19}	7.494×10^{-19}	3.714×10^{-19}
7	2.186×10^{-19}	9.197×10^{-19}	1.443×10^{-19}	7.618×10^{-19}	3.603×10^{-19}
8	2.267×10^{-19}	9.106×10^{-19}	1.443×10^{-19}	7.712×10^{-19}	3.518×10^{-19}
9	2.332×10^{-19}	9.033×10^{-19}	1.443×10^{-19}	7.787×10^{-19}	3.452×10^{-19}
10	2.385×10^{-19}	8.974×10^{-19}	1.443×10^{-19}	7.847×10^{-19}	3.398×10^{-19}
11	2.428×10^{-19}	8.926×10^{-19}	1.443×10^{-19}	7.896×10^{-19}	3.353×10^{-19}
12	2.465×10^{-19}	8.885×10^{-19}	1.443×10^{-19}	7.938×10^{-19}	3.316×10^{-19}
13	2.496×10^{-19}	8.850×10^{-19}	1.443×10^{-19}	7.973×10^{-19}	3.284×10^{-19}
14	2.523×10^{-19}	8.820×10^{-19}	1.443×10^{-19}	8.004×10^{-19}	3.257×10^{-19}
15	2.546×10^{-19}	8.794×10^{-19}	1.443×10^{-19}	8.030×10^{-19}	3.233×10^{-19}
16	2.567×10^{-19}	8.771×10^{-19}	1.443×10^{-19}	8.054×10^{-19}	3.212×10^{-19}
17	2.585×10^{-19}	8.751×10^{-19}	1.443×10^{-19}	8.074×10^{-19}	3.193×10^{-19}
18	2.602×10^{-19}	8.732×10^{-19}	1.443×10^{-19}	8.093×10^{-19}	3.177×10^{-19}
19	2.616×10^{-19}	8.716×10^{-19}	1.443×10^{-19}	8.109×10^{-19}	3.162×10^{-19}
20	2.630×10^{-19}	8.701×10^{-19}	1.443×10^{-19}	8.124×10^{-19}	3.149×10^{-19}
21	2.642×10^{-19}	8.688×10^{-19}	1.443×10^{-19}	8.138×10^{-19}	3.137×10^{-19}
22	2.653×10^{-19}	8.676×10^{-19}	1.443×10^{-19}	8.150×10^{-19}	3.126×10^{-19}
23	2.663×10^{-19}	8.665×10^{-19}	1.443×10^{-19}	8.161×10^{-19}	3.115×10^{-19}
24	2.672×10^{-19}	8.655×10^{-19}	1.443×10^{-19}	8.171×10^{-19}	3.106×10^{-19}
25	2.680×10^{-19}	8.645×10^{-19}	1.443×10^{-19}	8.181×10^{-19}	3.098×10^{-19}
26	2.688×10^{-19}	8.636×10^{-19}	1.443×10^{-19}	8.190×10^{-19}	3.090×10^{-19}
27	2.695×10^{-19}	8.628×10^{-19}	1.443×10^{-19}	8.198×10^{-19}	3.082×10^{-19}
28	2.702×10^{-19}	8.621×10^{-19}	1.443×10^{-19}	8.206×10^{-19}	3.075×10^{-19}
29	2.708×10^{-19}	8.614×10^{-19}	1.443×10^{-19}	8.213×10^{-19}	3.069×10^{-19}
30	2.714×10^{-19}	8.607×10^{-19}	1.443×10^{-19}	8.219×10^{-19}	3.063×10^{-19}

Table 3. Calculated NF b–X (0,0) Band Stimulated Emission Cross Section at 600 K (continued)

N	^{O}P Branch	^{Q}P Branch	^{Q}Q Branch	^{Q}R Branch	^{S}R Branch
31	2.720×10^{-19}	8.601×10^{-19}	1.443×10^{-19}	8.225×10^{-19}	3.058×10^{-19}
32	2.725×10^{-19}	8.595×10^{-19}	1.443×10^{-19}	8.231×10^{-19}	3.052×10^{-19}
33	2.730×10^{-19}	8.590×10^{-19}	1.443×10^{-19}	8.237×10^{-19}	3.048×10^{-19}
34	2.734×10^{-19}	8.585×10^{-19}	1.443×10^{-19}	8.242×10^{-19}	3.043×10^{-19}
35	2.739×10^{-19}	8.580×10^{-19}	1.443×10^{-19}	8.247×10^{-19}	3.039×10^{-19}
36	2.743×10^{-19}	8.575×10^{-19}	1.443×10^{-19}	8.251×10^{-19}	3.034×10^{-19}
37	2.747×10^{-19}	8.571×10^{-19}	1.443×10^{-19}	8.256×10^{-19}	3.031×10^{-19}
38	2.750×10^{-19}	8.567×10^{-19}	1.443×10^{-19}	8.260×10^{-19}	3.027×10^{-19}
39	2.754×10^{-19}	8.563×10^{-19}	1.443×10^{-19}	8.264×10^{-19}	3.023×10^{-19}
40	2.757×10^{-19}	8.559×10^{-19}	1.443×10^{-19}	8.267×10^{-19}	3.020×10^{-19}

Cross section in units of cm3/molecule

Table 4. Calculated NF b–X (0,0) Band Stimulated Emission Cross Section at 900 K

N	^{O}P Branch	^{Q}P Branch	^{Q}Q Branch	^{Q}R Branch	^{S}R Branch
2	6.942×10^{-20}	8.771×10^{-19}	1.178×10^{-19}	4.864×10^{-19}	4.127×10^{-19}
3	1.148×10^{-19}	8.233×10^{-19}	1.178×10^{-19}	5.459×10^{-19}	3.617×10^{-19}
4	1.410×10^{-19}	7.932×10^{-19}	1.178×10^{-19}	5.779×10^{-19}	3.335×10^{-19}
5	1.579×10^{-19}	7.741×10^{-19}	1.178×10^{-19}	5.980×10^{-19}	3.156×10^{-19}
6	1.697×10^{-19}	7.607×10^{-19}	1.178×10^{-19}	6.119×10^{-19}	3.032×10^{-19}
7	1.784×10^{-19}	7.510×10^{-19}	1.178×10^{-19}	6.220×10^{-19}	2.942×10^{-19}
8	1.851×10^{-19}	7.435×10^{-19}	1.178×10^{-19}	6.297×10^{-19}	2.873×10^{-19}
9	1.904×10^{-19}	7.376×10^{-19}	1.178×10^{-19}	6.358×10^{-19}	2.818×10^{-19}
10	1.947×10^{-19}	7.328×10^{-19}	1.178×10^{-19}	6.407×10^{-19}	2.774×10^{-19}
11	1.983×10^{-19}	7.288×10^{-19}	1.178×10^{-19}	6.447×10^{-19}	2.738×10^{-19}
12	2.013×10^{-19}	7.255×10^{-19}	1.178×10^{-19}	6.481×10^{-19}	2.708×10^{-19}
13	2.038×10^{-19}	7.226×10^{-19}	1.178×10^{-19}	6.510×10^{-19}	2.682×10^{-19}
14	2.060×10^{-19}	7.202×10^{-19}	1.178×10^{-19}	6.535×10^{-19}	2.659×10^{-19}
15	2.079×10^{-19}	7.180×10^{-19}	1.178×10^{-19}	6.557×10^{-19}	2.640×10^{-19}
16	2.096×10^{-19}	7.162×10^{-19}	1.178×10^{-19}	6.576×10^{-19}	2.623×10^{-19}
17	2.111×10^{-19}	7.145×10^{-19}	1.178×10^{-19}	6.593×10^{-19}	2.607×10^{-19}
18	2.124×10^{-19}	7.130×10^{-19}	1.178×10^{-19}	6.608×10^{-19}	2.594×10^{-19}
19	2.136×10^{-19}	7.117×10^{-19}	1.178×10^{-19}	6.621×10^{-19}	2.582×10^{-19}
20	2.147×10^{-19}	7.105×10^{-19}	1.178×10^{-19}	6.633×10^{-19}	2.571×10^{-19}
21	2.157×10^{-19}	7.094×10^{-19}	1.178×10^{-19}	6.644×10^{-19}	2.561×10^{-19}
22	2.166×10^{-19}	7.084×10^{-19}	1.178×10^{-19}	6.654×10^{-19}	2.552×10^{-19}
23	2.174×10^{-19}	7.075×10^{-19}	1.178×10^{-19}	6.664×10^{-19}	2.544×10^{-19}
24	2.181×10^{-19}	7.066×10^{-19}	1.178×10^{-19}	6.672×10^{-19}	2.536×10^{-19}
25	2.188×10^{-19}	7.059×10^{-19}	1.178×10^{-19}	6.680×10^{-19}	2.529×10^{-19}
26	2.195×10^{-19}	7.052×10^{-19}	1.178×10^{-19}	6.687×10^{-19}	2.523×10^{-19}
27	2.201×10^{-19}	7.045×10^{-19}	1.178×10^{-19}	6.694×10^{-19}	2.517×10^{-19}
28	2.206×10^{-19}	7.039×10^{-19}	1.178×10^{-19}	6.700×10^{-19}	2.511×10^{-19}
29	2.211×10^{-19}	7.033×10^{-19}	1.178×10^{-19}	6.706×10^{-19}	2.506×10^{-19}
30	2.216×10^{-19}	7.028×10^{-19}	1.178×10^{-19}	6.711×10^{-19}	2.501×10^{-19}

Table 4. Calculated NF b–X (0,0) Band Stimulated Emission Cross Section at 900 K (continued)

N	^{O}P Branch	^{Q}P Branch	^{Q}Q Branch	^{Q}R Branch	^{S}R Branch
31	2.221×10^{-19}	7.023×10^{-19}	1.178×10^{-19}	6.716×10^{-19}	2.497×10^{-19}
32	2.225×10^{-19}	7.018×10^{-19}	1.178×10^{-19}	6.721×10^{-19}	2.492×10^{-19}
33	2.229×10^{-19}	7.014×10^{-19}	1.178×10^{-19}	6.725×10^{-19}	2.488×10^{-19}
34	2.233×10^{-19}	7.009×10^{-19}	1.178×10^{-19}	6.729×10^{-19}	2.485×10^{-19}
35	2.236×10^{-19}	7.006×10^{-19}	1.178×10^{-19}	6.733×10^{-19}	2.481×10^{-19}
36	2.240×10^{-19}	7.002×10^{-19}	1.178×10^{-19}	6.737×10^{-19}	2.478×10^{-19}
37	2.243×10^{-19}	6.998×10^{-19}	1.178×10^{-19}	6.741×10^{-19}	2.474×10^{-19}
38	2.246×10^{-19}	6.995×10^{-19}	1.178×10^{-19}	6.744×10^{-19}	2.471×10^{-19}
39	2.249×10^{-19}	6.992×10^{-19}	1.178×10^{-19}	6.747×10^{-19}	2.469×10^{-19}
40	2.251×10^{-19}	6.989×10^{-19}	1.178×10^{-19}	6.750×10^{-19}	2.466×10^{-19}

Cross section in units of cm3/molecule

LABORATORY OPERATIONS

The Aerospace Corporation functions as an "architect-engineer" for national security projects, specializing in advanced military space systems. Providing research support, the corporation's Laboratory Operations conducts experimental and theoretical investigations that focus on the application of scientific and technical advances to such systems. Vital to the success of these investigations is the technical staff's wide-ranging expertise and its ability to stay current with new developments. This expertise is enhanced by a research program aimed at dealing with the many problems associated with rapidly evolving space systems. Contributing their capabilities to the research effort are these individual laboratories:

Aerophysics Laboratory: Launch vehicle and reentry fluid mechanics, heat transfer and flight dynamics; chemical and electric propulsion, propellant chemistry, chemical dynamics, environmental chemistry, trace detection; spacecraft structural mechanics, contamination, thermal and structural control; high temperature thermomechanics, gas kinetics and radiation; cw and pulsed chemical and excimer laser development, including chemical kinetics, spectroscopy, optical resonators, beam control, atmospheric propagation, laser effects and countermeasures.

Chemistry and Physics Laboratory: Atmospheric chemical reactions, atmospheric optics, light scattering, state-specific chemical reactions and radiative signatures of missile plumes, sensor out-of-field-of-view rejection, applied laser spectroscopy, laser chemistry, laser optoelectronics, solar cell physics, battery electrochemistry, space vacuum and radiation effects on materials, lubrication and surface phenomena, thermionic emission, photosensitive materials and detectors, atomic frequency standards, and environmental chemistry.

Electronics Research Laboratory: Microelectronics, solid-state device physics, compound semiconductors, radiation hardening; electro-optics, quantum electronics, solid-state lasers, optical propagation and communications; microwave semiconductor devices, microwave/millimeter wave measurements, diagnostics and radiometry, microwave/millimeter wave thermionic devices; atomic time and frequency standards; antennas, rf systems, electromagnetic propagation phenomena, space communication systems.

Materials Sciences Laboratory: Development of new materials: metals, alloys, ceramics, polymers and their composites, and new forms of carbon; nondestructive evaluation, component failure analysis and reliability; fracture mechanics and stress corrosion; analysis and evaluation of materials at cryogenic and elevated temperatures as well as in space and enemy-induced environments.

Space Sciences Laboratory: Magnetospheric, auroral and cosmic ray physics, wave-particle interactions, magnetospheric plasma waves; atmospheric and ionospheric physics, density and composition of the upper atmosphere, remote sensing using atmospheric radiation; solar physics, infrared astronomy, infrared signature analysis; effects of solar activity, magnetic storms and nuclear explosions on the earth's atmosphere, ionosphere and magnetosphere; effects of electromagnetic and particulate radiations on space systems; space instrumentation.